Chemical Science

ROYAL SOCIETY OF CHEMISTRY

EDGE ARTICLE

View Article Online
View Journal | View Issue

Cite this: *Chem. Sci.*, 2022, **13**, 4082

All publication charges for this article have been paid for by the Royal Society of Chemistry

State- and water repellency-controllable molecular glass of pillar[5]arenes with fluoroalkyl groups by guest vapors†

Katsuto Onishi, [a] Shunsuke Ohtani, [a] Kenichi Kato, [a] Shixin Fa, [a] Yoko Sakata, [bc] Shigehisa Akine, [bc] Moe Ogasawara, [c] Hitoshi Asakawa, [bcd] Shusaku Nagano, [e] Yoshinori Takashima, [fgh] Motohiro Mizuno [cd] and Tomoki Ogoshi *[ab]

Received 9th February 2022
Accepted 3rd March 2022

DOI: 10.1039/d2sc00828a

rsc.li/chemical-science

Molecular glasses are low-molecular-weight organic compounds that are stable in the amorphous state at room temperature. Herein, we report a state- and water repellency-controllable molecular glass by *n*-alkane guest vapors. We observed that a macrocyclic host compound pillar[5]arene with the C_2F_5 fluoroalkyl groups changes from the crystalline to the amorphous state (molecular glass) by heating above its melting point and then cooling to room temperature. The pillar[5]arene molecular glass shows reversible transitions between amorphous and crystalline states by uptake and release of the *n*-alkane guest vapors, respectively. Furthermore, the *n*-alkane guest vapor-induced reversible changes in the water contact angle were also observed: water contact angles increased and then reverted back to the original state by the uptake and release of the *n*-alkane guest vapors, respectively, along with the changes in the chemical structure and roughness on the surface of the molecular glass. The water repellency of the molecular glass could be controlled by tuning the uptake ratio of the *n*-alkane guest vapor.

Introduction

Low molecular weight organic compounds are generally easy-to-crystalize compared with high-molecular-weight organic compounds. Design of low-molecular-weight organic glasses, which form stable amorphous states even at room temperature, is an interesting research area as they are superior to high-molecular-weight organic glasses in terms of transparency, homogeneity and film-forming properties.[1,2] Owing to these properties, organic glasses have been used as organic light-emitting diodes and resist materials.[3–8] One of the molecular designs to create organic molecular glasses is introduction of non-planar structures. For example, molecules with twisted small π-units such as triphenylamine and tetraphenylmethane derivatives can be organic molecular glasses, as these skeletons are non-planar structures with diverse molecular conformations, which prevent the ordered periodic crystalline assemblies.[5,9] Introducing bulky groups and/or intermolecular interactions is another design strategy to obtain molecular glasses.[10] Furthermore, design of stimuli-responsive functional molecular glasses, which can easily exchange amorphous–crystalline states by external stimuli and exhibit new functions resulting from the stimuli-responsive transitions, is the next challenge. Until now, only photo-responsive molecular glass with an azobenzene group showing an amorphous–crystalline transition has been reported.[11]

Pillar[*n*]arenes, which were reported by our group in 2008,[12] are highly symmetrical pillar-shaped macrocyclic host molecules. After their discovery, pillar[*n*]arenes became key players in supramolecular chemistry due to their superior functionalities, host–guest properties and unique pillar-shaped structures.[13–18] In most cases, pillar[*n*]arenes form crystalline solids

[a]*Department of Synthetic Chemistry and Biological Chemistry, Graduate School of Engineering, Kyoto University, Katsura, Nishikyo-ku, Kyoto 615-8510, Japan. E-mail: ogoshi@sbchem.kyoto-u.ac.jp*

[b]*WPI Nano Life Science Institute (WPI-NanoLSI), Kanazawa University, Kakuma-machi, Kanazawa, Ishikawa, 920-1192, Japan*

[c]*Graduate School of Natural Science and Technology, Kanazawa University, Kakuma-machi, Kanazawa, 920-1192, Japan*

[d]*Nanomaterials Research Institute, Kanazawa University, Kakuma-machi, Kanazawa, 920-1192, Japan*

[e]*Department of Chemistry, College of Science, Rikkyo University, 3-34-1 Nishi-Ikebukuro, Toshima, Tokyo, 171-8501, Japan*

[f]*Department of Macromolecular Science, Graduate School of Science and Project Research Center for Fundamental Sciences, Graduate School of Science, Osaka University, Toyonaka, Osaka 560-0043, Japan*

[g]*Institute for Advanced Co-Creation Studies, Osaka University, Suita, Osaka 565-0871, Japan*

[h]*Innovative Catalysis Science Division, Institute for Open and Transdisciplinary Research Initiatives (OTRI), Osaka University, Suita, Osaka 565-0871, Japan*

† Electronic supplementary information (ESI) available: Experimental procedures, NMR, UV-vis spectra, single-crystal X-ray structural analysis, PXRD, gas adsorption, DSC, TGA, contact angle and movie. CCDC 2121263–2121267 and 2144343. For ESI and crystallographic data in CIF or other electronic format see DOI: 10.1039/d2sc00828a

at room temperature due to their highly symmetrical pillar-shaped structures and crystalline solids form host–guest complexes by exposure to *n*-alkane guest vapors.[19–26] Moreover, an important feature of pillar[5]arenes is their high functionalities;[27] they have 10 reaction sites, meaning that various functional groups can be installed. The functional groups on both the rims significantly affect the physical properties of pillar[5]arenes.[28,29] In this study, we discovered that a pillar[5]arene with C_2F_5 fluoroalkyl groups on both rims could be a molecular glass. As in crystalline pillar[*n*]arenes, the transparent amorphous molecular glass took up *n*-alkane guest vapors by exposure to the vapors. Interestingly, the uptake caused an appearance change from transparent to turbid films due to the formation of the crystalline structure. The turbid film reverted back to the transparent film again by removing the guest through heating. The amorphous to crystalline and crystalline to amorphous state transitions were completely reversible by the uptake and release of the guest vapors, respectively. The guest vapor-responsive transitions were not observed in pillar[5]arenes with short and long fluoroalkyl groups, thus the transitions can be achieved by installing the C_2F_5 fluoroalkyl groups. Furthermore, based on the guest vapor-responsive transitions, switching and tuning of the water repellency could be demonstrated.

Results and discussion

Syntheses and phase changes of pillar[5]arenes with fluoroalkyl groups

We synthesized pillar[5]arene derivatives with various lengths of fluoroalkyl groups and a compound with no fluorine atoms (**F5**, **F3**, **F13** and **C5** in Fig. 1a). Pillar[6]arene with C_2F_5 groups (**[6]F5**) and a **Monomer Unit** with no macrocyclic structure were also synthesized.[30] All new compounds were characterized by ^{1}H, ^{13}C and ^{19}F NMR spectroscopy and mass spectrometry (details in the ESI†).

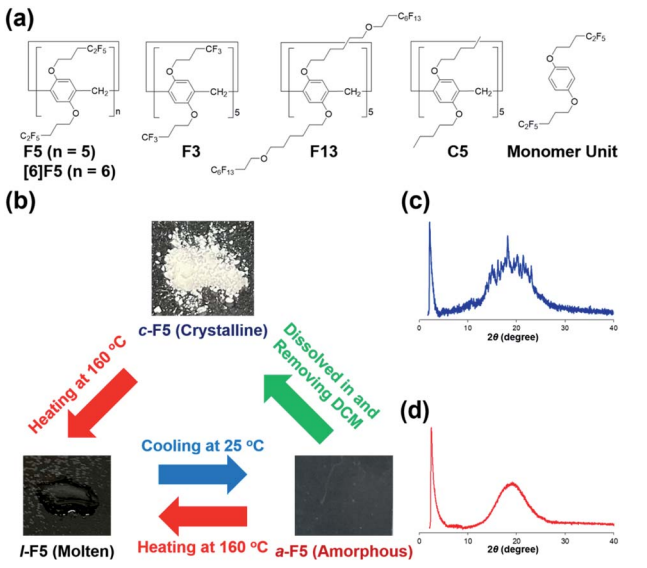

Fig. 1 (a) Chemical structures of F5, [6]F5, F3, C5, F13 and the Monomer Unit. (b) Photographs of *c*-F5, *l*-F5 and *a*-F5. PXRD patterns of (c) *c*-F5 and (d) *a*-F5.

F5 exhibits three states as shown in Fig. 1b. Initially, white solid **F5** was obtained at 25 °C after evaporation of dichloromethane (DCM) containing **F5**. The solid contained no solvents, which was confirmed by ^{1}H NMR (Fig. S16†). Powder X-ray diffraction (PXRD) measurement (Fig. 1c) of the solid showed many sharp peaks, which suggested that the solid **F5** existed in the crystalline state (denoted as ***c*-F5**). From differential scanning calorimetry (DSC), the melting point of ***c*-F5** was 116 °C (Fig. S17†), thus ***c*-F5** became a viscous liquid (denoted as ***l*-F5**, Fig. 1b) when heated to 160 °C. Unexpectedly, by cooling, ***l*-F5** did not go back to the pristine white crystalline solid ***c*-F5**, but a new state, transparent film. In PXRD measurement (Fig. 1d), the transparent film did not show sharp peaks, indicating that it was an amorphous solid, *i.e.*, an organic molecular glass (denoted as ***a*-F5**). The phase transition was completely reversible. ***a*-F5** changed to ***l*-F5** on heating at 160 °C and then reverted back to ***a*-F5** after cooling to 25 °C. ***a*-F5** could also change to ***c*-F5** by dissolving ***a*-F5** in DCM, and then completely removing the solvent under reduced pressure at 60 °C. In contrast to **F5**, these three states were not observed in **F3** with short CF_3 groups, **C5** with no fluorine atoms, **F13** with long C_6F_{13} groups and the **Monomer Unit** with no macrocyclic structure by heating and then cooling treatments (details in Fig. S18 and S19†).[31] To investigate the effect of the C_2F_5 groups, we also prepared pillar[6]arene with C_2F_5 groups (**[6]F5**). Like **F5**, **[6]F5** became a molecular glass (details in Fig. S20†). Therefore, the installation of the C_2F_5 groups into pillar[*n*]arene enabled the reversible changes between crystalline and amorphous phases, which are rare in macrocyclic compounds.[31,32] To understand the effect of the C_2F_5 groups on formation of molecular glasses, DFT calculations were performed (Fig. S30†). From molecular electrostatic potential maps, **F5** had little differences in the electron density distribution between both the rims and the cavity. On the other hand, electron-poor rims and electron-rich cavity were observed in typical pillar[5]arenes with methoxy groups. These results suggested that **F5** was unlikely to form the ordered structure through intermolecular C–H$\cdots\pi$ and π–π interactions as observed in typical crystalline pillar[5]arenes. Thus, even in the highly symmetrical pillar-shaped structure of pillar[*n*]arenes, the organic molecular glasses can be produced by installing the C_2F_5 fluoroalkyl groups.

Guest vapor-responsive state transitions

It is known that crystalline pillar[5]arenes take up *n*-alkane guest vapors in their cavities.[15,18] Therefore, we exposed ***a*-F5** to *n*-hexane vapors. ***a*-F5** took up *n*-hexane vapors in 1 : 1 host : guest ratio, which was checked by ^{1}H NMR (Fig. S21†). Interestingly, ***a*-F5** changed from a transparent film to a turbid film by exposure to *n*-hexane vapors (Fig. 2a). The appearance change occurred within only several minutes; thus, we could visually follow the events (Movie S1†). More interestingly, the change was completely reversible: ***c*-(F5⊃H)** returned to a transparent film ***a*-F5** by heating at 160 °C and then cooling to 25 °C, and the resulting transparent film changed to a turbid

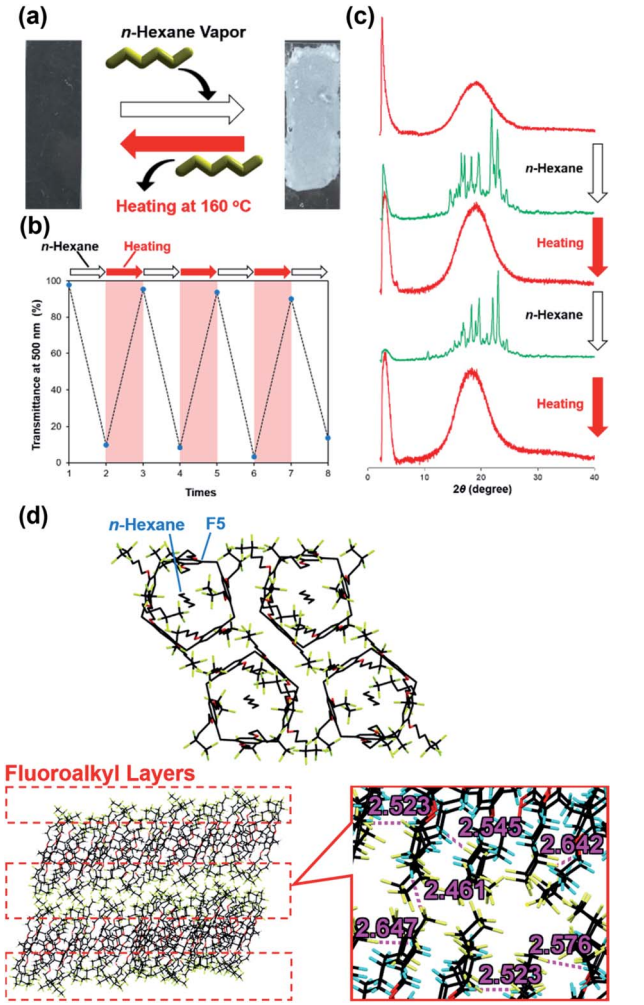

Fig. 2 (a) Photographs, (b) transmittance changes at 500 nm and (c) PXRD patterns of **F5** by exposing ***a*-F5** to *n*-hexane vapors for 17 h and heating ***c*-(F5⊃H)** at 160 °C within 1 minute. (d) Single-crystal structures of **F5⊃H**; all labeled distances of intermolecular C–H···F hydrogen bonds are given in the order of angstrom. F, O, C and H atoms are represented by yellow, red, black and light blue capped sticks, respectively.

film by exposure to *n*-hexane vapors again (Fig. 2a). We monitored the transitions by UV-vis transmittance spectroscopy, showing the transmittance change between around 98% (***a*-F5**) and 10% (***c*-(F5⊃H)**) (Fig. 2b and Table S1†). The reversible appearance changes were caused by the transitions between amorphous and crystalline states. From PXRD measurements (Fig. 2c), the reversible transitions between amorphous and crystalline states by uptake and release of *n*-hexane vapors could be confirmed. Contrary to **F5**, the appearance change induced by exposure to *n*-hexane guest vapors was not observed in any of the reference compounds, *i.e.*, **F3**, **C5**, **F13** and the **Monomer Unit** (Fig. S22†).

F3, **C5** and the **Monomer Unit** were crystalline states both before and after exposure to *n*-hexane vapors, indicating that amorphous state ***a*-F5** was successfully obtained by the installation of more fluorine atoms on the side chains of pillar[5]arenes. On the other hand, **F13** remained in the amorphous state even after the exposure to vapors, suggesting that aggregation of the long C_6F_{13} groups in **F13** inhibited the state transition. These results concluded that the installation of the C_2F_5 groups enabled **F5** to form amorphous state ***a*-F5** and the vapor-induced amorphous to crystalline transitions. The C_2F_5 groups also allowed amorphous **[6]F5** to be in the crystalline state by exposure to cyclohexane vapors (Fig. S42†), indicating that the C_2F_5 groups are good substituents to produce the guest vapor-responsive pillar[*n*]arene molecular glasses.

To reveal the roles of the C_2F_5 groups in ***c*-(H⊃F5)**, we obtained single crystals of **F5** from chloroform under *n*-hexane vapors (**F5⊃H**). From single-crystal X-ray structural analysis (Fig. 2d), **F5** formed a 1 : 1 host–guest complex with *n*-hexane, corresponding to the aforementioned ^{1}H NMR study of ***c*-(F5⊃H)** (Fig. S21†). The complex formed a highly symmetrical pillar-shaped structure, resulting in the formation of one-dimensional channel assemblies. Fluoroalkyl layer formation was induced by intermolecular C–H···F hydrogen bonds. The PXRD pattern simulated from a single crystal of **F5⊃H** was close to that of ***c*-(F5⊃H)** (Fig. S28†), indicating that the assembled structure of ***c*-(F5⊃H)** was similar to that of a single crystal of **F5⊃H**.

To obtain the structural information of ***a*-F5**, we performed solid-state ^{13}C NMR (Fig. S29†). Obvious peak shifts of the carbon signals from the fluoroalkyl groups of **F5** were observed in the samples before and after exposure to *n*-hexane vapors, indicating that the structure of the fluoroalkyl groups mainly changed along with the transition from ***a*-F5** to ***c*-(F5⊃H)**.

We investigated the uptake of other organic vapors by ***a*-F5** from ^{1}H NMR measurements (Fig. S31–S35†). ***a*-F5** took up organic guest vapors such as *n*-pentane, methanol, ethanol, toluene and 1,4-dicyanobutane. The uptake of these organic guest vapors triggered amorphous to crystalline transitions (Fig. S36†) and it only took several minutes for the state transitions to begin as in the case of *n*-hexane. Solubilization of ***a*-F5** was observed by exposing ***a*-F5** to DCM, 1,2-dichloroethane and chloroform vapors, which are good solvents for **F5**.

Guest vapor-responsive water contact angles

Because the *n*-hexane guest vapor uptake triggered the formation of the fluoroalkyl layers, we measured the water contact angles. Fig. 3a shows the change of the water contact angle along with the state transition of **F5** by the complexation. By the *n*-hexane vapor uptake, the contact angle value increased from 98 ± 3° (***a*-F5**) to 112 ± 1°(***c*-(F5⊃H)**).

We also measured the contact angles of other complexes composed of **F5** with *n*-pentane, methanol, ethanol, toluene and 1,4-dicyanobutane (Table S2†). Apart from the complex of **F5** with *n*-pentane (***c*-(F5⊃P)**), none of the complexes showed as much increase in the contact angles as ***c*-(F5⊃H)**. Surprisingly, *n*-pentane vapors dramatically increased the contact angle value to 119 ± 2° (Fig. 3a), which is higher than that of ***c*-(F5⊃H)** (112 ± 1°) and unmodified polytetrafluoroethylene (114°).[33]

In general, the increase in water repellency can be ascribed to two main factors: one is the increased hydrophobicity of the surface chemical structure and the other is the increased

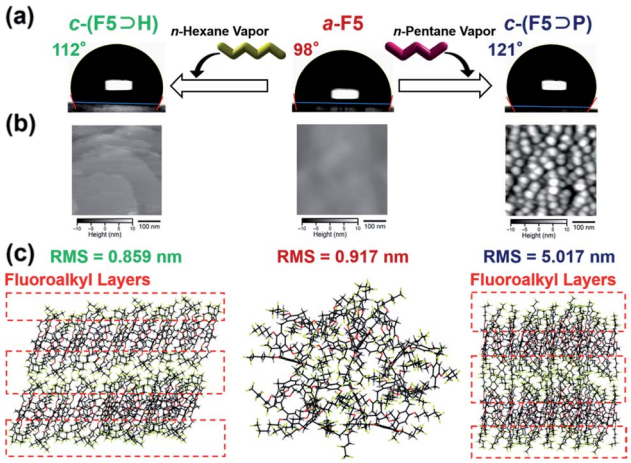

Fig. 3 (a) Water contact angle changes of F5 by exposing ***a*-F5** (middle) to *n*-hexane (left) or *n*-pentane (right) vapors. (b) AFM images of ***a*-F5** (middle), **F5⊃H** (left) and **F5⊃P** (right). Range of grey scales: 20 nm. Size of AFM images: 400 × 400 nm^2. (c) Single-crystal structures of **F5⊃H** (left) and **F5⊃P** (right); F, O and C atoms are represented by yellow, red and black capped sticks, respectively. Hydrogen atoms and *n*-hexane guest molecules are omitted for clarity. The assembled structure of ***a*-F5** (middle) was proposed from the results of solid-state ^{13}C NMR and DFT calculations.

surface roughness.[34–38] To elucidate these factors, we performed single-crystal X-ray structural analysis and atomic force microscopy (AFM) analysis to investigate the chemical structure and roughness on the surface, respectively.

It is again noted that the fluoroalkyl layers were formed in the ***c*-(F5⊃H)** structure. A similar fluoroalkyl layer formation induced by C–H···F interactions was also observed in single-crystal X-ray structural analysis (Fig. 3c and S37†) of **F5⊃P**, which were obtained in a mixture of chloroform and *n*-pentane. AFM analysis (Fig. 3b) of ***c*-(F5⊃H)** showed flat terraces with 1 nm thickness attributed to a layer structure on the crystalline surfaces perpendicular to the glass substrate. The root mean square (RMS) value of ***a*-F5** (0.917 nm) was similar to that of ***c*-(F5⊃H)** (0.859 nm), indicating that surface roughness did not change clearly even after the assembled structure change induced by *n*-hexane vapors. Contrary to this, in the case of ***c*-(F5⊃P)**, there were many crystallites on the surface and the RMS value of ***c*-(F5⊃P)** was 5.017 nm, suggesting a rougher surface compared with those of ***a*-F5** and ***c*-(F5⊃H)**. These results indicated that different reasons contributed to these increases in the water contact angles: in the case of *n*-hexane guest vapors, the main reason is the formation of fluoroalkyl layers. In the case of *n*-pentane, not only the formation of fluoroalkyl layers but also the increase in surface roughness resulted in the increase. Therefore, a greater increase was observed in the contact angle of ***c*-(F5⊃P)** than that of ***c*-(F5⊃H)** (Fig. 3). Oil repellency of ***a*-F5**, ***c*-(F5⊃H)** and ***c*-(F5⊃P)** also supported this explanation (detailed discussion in Table S3†). Overall, changes in macroscopic physical properties such as water and oil repellency were achieved along with the amorphous–crystalline transitions by uptake and release of the guest vapors. In contrast to these results, reference compounds **F3**, **C5**, **F13** and the **Monomer Unit** showed a small change in water contact angles even after exposure to *n*-hexane or *n*-pentane vapors and the contact angles were lower than those of ***c*-(F5⊃H)** and ***c*-(F5⊃P)** (Table S4†). This indicated that the number of fluorine atoms on the rims of pillar[5]arenes and the formation of the fluoroalkyl layers by the guest vapor uptake are important factors for the increase in the contact angles (detailed discussion in Fig. S57†).

Water repellency control by uptake of *n*-pentane guest vapors

As in the case of reversible state transitions by *n*-hexane vapors, crystalline ***c*-(F5⊃P)** returned to amorphous ***a*-F5** by the release of *n*-pentane guest vapors on heating at 160 °C. Exposure to *n*-pentane vapors again reverted ***a*-F5** back to ***c*-(F5⊃P)** by uptake of *n*-pentane vapors. The *n*-pentane guest vapor-triggered reversible amorphous–crystalline and transmittance changes were confirmed by PXRD measurements (Fig. S38†) and UV-vis transmittance spectroscopy (Fig. S39†), respectively. Furthermore, the contact angles were reversibly changed between approximately 98° and 120° by uptake and release of *n*-pentane vapors (Fig. S40†).[39] These results indicated that the contact angles of **F5** reversibly changed based on the state transitions by the uptake and release of *n*-pentane vapors.

By tuning the exposure time to that of *n*-pentane vapors, gradual *n*-pentane uptake in ***a*-F5** was observed, which was monitored by ^{1}H NMR measurements (Table S5 and Fig. S44†). There was a plateau after 1 h exposure to *n*-pentane vapors (Fig. 4), indicating that *n*-pentane uptake by ***a*-F5** had reached a saturated state only by 1 h exposure. Thus, we investigated the relationship between the uptake ratio of *n*-pentane to **F5** and the water repellency (Fig. 4 and Table S6†). Contact angle measurements showed that a longer exposure time of 1 h allowed the contact angles to increase gradually from 98° to around 120°, which corresponded to the contact angle of the saturated state ***c*-(F5⊃P)**. Therefore, contact angles of ***a*-F5** were tuned by controlling the uptake ratio of *n*-pentane. From UV-vis

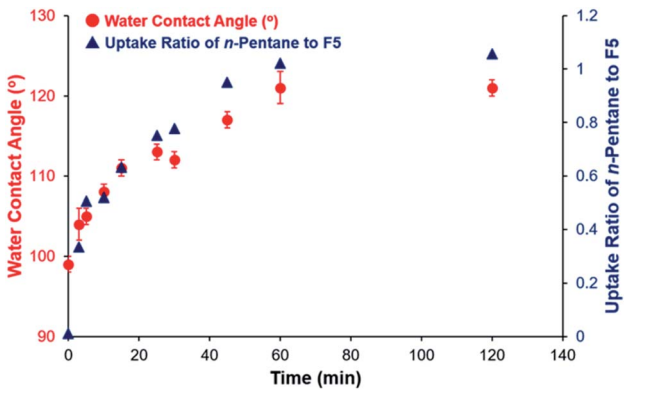

Fig. 4 Time-dependent changes in uptake ratios of *n*-pentane to ***a*-F5** (blue triangles) and water contact angles (red circles). The uptake ratios were calculated by ^{1}H NMR measurements. The error bars represent one standard error from five independent measurements.

transmittance spectroscopy, it can be observed that transmittance decreased gradually as the exposure time was longer (Fig. S45 and Table S7†), suggesting that ***a*-F5** also showed exposure time-dependent appearance change from transparent to turbid states.

To understand these mechanisms, we investigated time-dependent changes in the formation of the crystalline structure by PXRD measurements and AFM analyses (Fig. S46 and S47†). From PXRD measurements, gradual appearances of sharp diffraction peaks were observed along with increasing ratio of *n*-pentane vapors, suggesting that amorphous to crystalline transitions of **F5** gradually occurred by *n*-pentane vapor uptake. From AFM analyses, it can be observed that crystalline structures with clear edges were gradually formed by exposure to *n*-pentane vapors, which was consisted with the PXRD results.

Conclusions

We observed that a pillar[5]arene with C_2F_5 fluoroalkyl groups could be an organic molecular glass as a transparent film by cooling the isotropic molten liquid of pillar[5]arene. Quite distinct from typical molecular glasses, the pillar[5]arene molecular glass showed guest vapor-responsive amorphous–crystalline transitions because it has a cavity to capture the guest vapors based on the host–guest system. By exposing the transparent film to the guest vapors, the transparent film changed to a turbid film by complexation with the guest vapors. In addition, release of the guest vapors by heating triggered the crystalline to amorphous transition. Taken together, completely reversible amorphous–crystalline state transitions occurred by the uptake and release of the guest vapors. There are a few examples of amorphous macrocyclic compounds,[31,32,40–42] but investigation of these amorphous macrocyclic compounds in terms of their macroscopic property changes was not reported. Vapochromism is a color/fluorescence change which occurs by exposing crystals to vapors.[43–45] In this study, *n*-alkane vapors can be directly monitored by the transparency changes of the film. Alkane vapor-responsive materials are very rare[46] because it is difficult for the C–H and C–C groups in alkanes to form stable interactions with adsorption materials. The transparent-turbid changes come from amorphous–crystalline state transitions by uptake and release of the guest vapors. The amorphous–crystalline transitions triggered a macroscopic property change such as water repellency. Uptake and release of the guest vapors cause changes in the chemical structure and roughness on the surface, enabling control of the contact angle. Another macroscopic property, adhesiveness, is also highly related to the chemical structure and roughness on the surface, thus both these changes demonstrated in this study along with amorphous–crystalline transitions will be applied to switchable adhesive materials. Coating materials for selective vapor uptake would also be another idea for the application of the pillar[5]arene molecular glass because pillar[5]arenes can capture *n*-alkane guest vapors and molecular glasses can be integrated in polymer and glass coatings.

Data availability

All relevant data are presented in the main text and ESI.†

Author contributions

T. O. conceptualized and supervised the work. K. O., S. O., K. K., S. F., Y. S., S. A., M. O., H. A., S. N., Y. T. and M. M. designed and performed experiments. The first draft of the manuscript was written by K. O. and T. O. All authors contributed to manuscript review.

Conflicts of interest

There are no conflicts to declare.

Acknowledgements

This work was supported by the Grant-in-Aid for Scientific Research on Innovative Areas: π-System Figuration (JP15H00990 and JP17H05148, T.O.), Soft Crystals (JP18H04510 and JP20H04670, T.O., JP18H04511 and JP 20H04667, Y.S., JP20H04666, M.M.), and K.A. (JP19H00909, T.O.) from MEXT Japan, JST CREST (JPMJCR18R3, T.O.), and the World Premier International Research Center Initiative (WPI), MEXT, Japan. This work was partially supported by Kanazawa University JIKOCHOKOKU project (H.A.).

Notes and references

1 Y. Shirota, *J. Mater. Chem.*, 2000, **10**, 1–25.
2 Y. Shirota, *J. Mater. Chem.*, 2005, **15**, 75–93.
3 L.-H. Chan, R.-H. Lee, C.-F. Hsieh, H.-C. Yeh and C.-T. Chen, *J. Am. Chem. Soc.*, 2002, **124**, 6469–6479.
4 A. De Silva, N. M. Felix and C. K. Ober, *Adv. Mater.*, 2008, **20**, 3355–3361.
5 J. Chen, Q. Hao, S. Wang, S. Li, T. Yu, Y. Zeng, J. Zhao, S. Yang, Y. Wu, C. Xue, G. Yang and Y. Li, *ACS Appl. Polym. Mater.*, 2019, **1**, 526–534.
6 D. Umeyama, S. Horike, M. Inukai, T. Itakura and S. Kitagawa, *J. Am. Chem. Soc.*, 2015, **137**, 864–870.
7 T. D. Bennett and S. Horike, *Nat. Rev. Mater.*, 2018, **3**, 431–440.
8 T. Ogawa, K. Takahashi, S. S. Nagarkar, K. Ohara, Y.-L. Hong, Y. Nishiyama and S. Horike, *Chem. Sci.*, 2019, **11**, 5175–5181.
9 M. Miyasaka, A. Rajca, M. Pink and S. Rajca, *Chem.–Eur. J.*, 2004, **10**, 6531–6539.
10 Y. Kasahara, I. Hisaki, T. Akutagawa and T. Takeda, *Chem. Commun.*, 2021, **57**, 5374–5377.
11 H. Umezawa, J.-M. Nunzi, O. Lebel and R. G. Sabat, *Langmuir*, 2016, **32**, 5646–5652.
12 T. Ogoshi, S. Kanai, S. Fujinami, T. Yamagishi and Y. Nakamoto, *J. Am. Chem. Soc.*, 2008, **130**, 5022–5023.
13 T. Ogoshi, T. Yamagishi and Y. Nakamoto, *Chem. Rev.*, 2016, **116**, 7937–8002.
14 M. Xue, Y. Yang, X. D. Chi, Z. B. Zhang and F. Huang, *Acc. Chem. Res.*, 2012, **45**, 1294–1308.

15 N. Song, T. Kakuta, T. Yamagishi, Y.-W. Yang and T. Ogoshi, *Chem*, 2018, **4**, 2029–2053.
16 W. Si, P. Xin, Z.-T. Li and J.-L. Hou, *Acc. Chem. Res.*, 2015, **48**, 1612–1619.
17 X.-Q. Wang, W.-J. Li, W. Wang and H. B. Yang, *Acc. Chem. Res.*, 2021, **54**, 4091–4106.
18 X.-Y. Lou and Y.-W. Yang, *Adv. Mater.*, 2020, **32**, 2003263.
19 T. Ogoshi, R. Sueto, K. Yoshikoshi, Y. Sakata, S. Akine and T. Yamagishi, *Angew. Chem., Int. Ed.*, 2015, **54**, 9849–9852.
20 T. Ogoshi, R. Sueto, Y. Hamada, K. Doitomi, H. Hirao, Y. Sakata, S. Akine, T. Kakuta and T. Yamagishi, *Chem. Commun.*, 2017, **53**, 8577–8580.
21 K. Jie, Y. Zhou, E. Li and F. Huang, *Acc. Chem. Res.*, 2018, **51**, 2064–2072.
22 T. Ogoshi, R. Sueto, M. Yagyu, R. Kojima, T. Kakuta, T. Yamagishi, K. Doitomi, A. K. Tummanapelli, H. Hirao, Y. Sakata, S. Akine and M. Mizuno, *Nat. Commun.*, 2019, **10**, 479.
23 J.-R. Wu and Y.-W. Yang, *Angew. Chem., Int. Ed.*, 2021, **60**, 1690–1701.
24 M. Wang, Q. Li, E. Li, J. Liu, J. Zhou and F. Huang, *Angew. Chem., Int. Ed.*, 2021, **60**, 8115–8120.
25 B. Li, S. Li, B. Wang, Z. Meng, Y. Wang, Q. Meng and C. Li, *iScience*, 2020, **23**, 101443.
26 W. Yang, K. Samanta, X. Wan, T. U. Thikekar, Y. Chao, S. Li, K. Du, J. Xu, Y. Gao, H. Zuilhof and A. C.-H. Sue, *Angew. Chem., Int. Ed.*, 2020, **59**, 3994–3999.
27 N. L. Strutt and H. C. Zhang, *Acc. Chem. Res.*, 2014, **47**, 2631–2642.
28 T. Ogoshi, T. Aoki, R. Shiga, R. Iizuka, S. Ueda, K. Demachi, D. Yamafuji, H. Kayama and T. Yamagishi, *J. Am. Chem. Soc.*, 2012, **134**, 20322–20325.
29 T. Ogoshi, K. Maruyama, Y. Sakatsume, T. Kakuta, T. Yamagishi, T. Ichikawa and M. Mizuno, *J. Am. Chem. Soc.*, 2019, **141**, 785–789.
30 We tried to synthesize pillar[5]arenes with various fluoroalkyl groups more than C_3F_7. In these cases, unfortunately, due to the low reactivity, we obtained starting compound, per-hydroxylated pillar[5]arene, indicating that introducing the longer fluoroalkyl groups was quite difficult.
31 K. Wada, T. Kakuta, T. Yamagishi and T. Ogoshi, *Chem. Commun.*, 2020, **56**, 4344–4347.
32 H. Yao, Y.-M. Wang, M. Quan, M. U. Farooq, L.-P. Yang and W. Jiang, *Angew. Chem., Int. Ed.*, 2020, **59**, 19945–19950.
33 T. Takahashi, Y. Hirano, Y. Takasawa, T. Gowa, N. Fukutake, A. Oshima, S. Tagawa and M. Washio, *Radiat. Phys. Chem.*, 2011, **80**, 253–256.
34 N. Nishikawa, H. Kiyohara, S. Sakiyama, S. Yamazoe, H. Mayama, T. Tsujioka, Y. Kojima, S. Yokojima, S. Nakamura and K. Uchida, *Langmuir*, 2012, **28**, 17817–17824.
35 B. Zhao, W. J. Brittain, W. Zhou and S. Z. D. Cheng, *J. Am. Chem. Soc.*, 2000, **122**, 2407–2408.
36 N. Vandencasteele, B. Broze, S. Collette, C. De Vos, P. Viville, R. Lazzaroni and F. Reniers, *Langmuir*, 2010, **26**, 16503–16509.
37 T. Onda, S. Shibuichi, N. Satoh and K. Tsujii, *Langmuir*, 1996, **12**, 2125–2127.
38 T. Sun, G. Wang, L. Feng, B. Liu, Y. Ma, L. Jiang and D. Zhu, *Angew. Chem., Int. Ed.*, 2004, **43**, 357–360.
39 *n*-Hexane guest vapor-induced reversible water contact angle changes were also observed (Fig. S41†).
40 K. Jie, Y. Zhou, E. Li, Z. Li, R. Zhao and F. Huang, *J. Am. Chem. Soc.*, 2017, **139**, 15320–15323.
41 J.-R. Wu, B. Li and Y.-W. Yang, *Angew. Chem., Int. Ed.*, 2020, **59**, 2251–2255.
42 J.-R. Wu, Z. Cai, G. Wu, D. Dai, Y.-Q. Liu and Y.-W. Yang, *J. Am. Chem. Soc.*, 2021, **143**, 20395–20402.
43 O. S. Wenger, *Chem. Rev.*, 2013, **113**, 3686–3733.
44 Q. Li, H. Zhu and F. Huang, *J. Am. Chem. Soc.*, 2019, **141**, 13290–13294.
45 X.-Y. Lou and Y.-W. Yang, *J. Am. Chem. Soc.*, 2021, **143**, 11976–11981.
46 T. Ogoshi, Y. Shimada, Y. Sakata, S. Akine and T. Yamagishi, *J. Am. Chem. Soc.*, 2017, **139**, 5664–5667.